

RESEARCH ARTICLE | *Central Pattern Generators*

Rhythm generation, coordination, and initiation in the vocal pathways of male African clawed frogs

Ayako Yamaguchi, Jessica Cavin Barnes, and Todd Appleby

Department of Biology, University of Utah, Salt Lake City, Utah

Submitted 8 August 2016; accepted in final form 15 October 2016

Yamaguchi A, Cavin Barnes J, Appleby T. Rhythm generation, coordination, and initiation in the vocal pathways of male African clawed frogs. *J Neurophysiol* 117: 178–194, 2017. First published October 19, 2016; doi:10.1152/jn.00628.2016.—Central pattern generators (CPGs) in the brain stem are considered to underlie vocalizations in many vertebrate species, but the detailed mechanisms underlying how motor rhythms are generated, coordinated, and initiated remain unclear. We addressed these issues using isolated brain preparations of *Xenopus laevis* from which fictive vocalizations can be elicited. Advertisement calls of male *X. laevis* that consist of fast and slow trills are generated by vocal CPGs contained in the brain stem. Brain stem central vocal pathways consist of a premotor nucleus [dorsal tegmental area of medulla (DTAM)] and a laryngeal motor nucleus [a homologue of nucleus ambiguus (n.IX-X)] with extensive reciprocal connections between the nuclei. In addition, DTAM receives descending inputs from the extended amygdala. We found that unilateral transection of the projections between DTAM and n.IX-X eliminated premotor fictive fast trill patterns but did not affect fictive slow trills, suggesting that the fast and slow trill CPGs are distinct; the slow trill CPG is contained in n.IX-X, and the fast trill CPG spans DTAM and n.IX-X. Midline transections that eliminated the anterior, posterior, or both commissures caused no change in the temporal structure of fictive calls, but bilateral synchrony was lost, indicating that the vocal CPGs are contained in the lateral halves of the brain stem and that the commissures synchronize the two oscillators. Furthermore, the elimination of the inputs from extended amygdala to DTAM, in addition to the anterior commissure, resulted in autonomous initiation of fictive fast but not slow trills by each hemibrain stem, indicating that the extended amygdala provides a bilateral signal to initiate fast trills.

NEW & NOTEWORTHY Central pattern generators (CPGs) are considered to underlie vocalizations in many vertebrate species, but the detailed mechanisms underlying their functions remain unclear. We addressed this question using an isolated brain preparation of African clawed frogs. We discovered that two vocal phases are mediated by anatomically distinct CPGs, that there are a pair of CPGs contained in the left and right half of the brain stem, and that mechanisms underlying initiation of the two vocal phases are distinct.

central pattern generator; vocalization; parabrachial area; hindbrain; bilateral coordination; motor programs

MANY RHYTHMIC MOTOR programs, including locomotion, breathing, and chewing behavior, are generated by central pattern generators (CPGs), neural circuits that can function without

rhythmic descending inputs or afferent feedback (Grillner 2006; Marder and Bucher 2001; Marder and Calabrese 1996). To understand the functions of CPGs, it is critical to identify neuronal components that make up CPGs, how they are coordinated, and in the case of episodic behavior, how CPG activity is initiated. Much effort to understand mechanisms underlying CPG function has been aided by the use of fictive preparations, in vitro preparations from which patterned neuronal activity that underlies rhythmic motor programs can be elicited (Sweeney and Kelley 2014). For example, fictive swimming (Buchanan 2011; Fetcho and McLean 2010; Roberts et al. 2012), walking (Kiehn et al. 2010), breathing (Garcia et al. 2011), and chewing (Marder et al. 2005) preparations played critical roles in advancing the understanding of the neural mechanisms of CPGs underlying these rhythmic behaviors.

Vocalizations produced by vertebrates are often rhythmic and are thought to be mediated by CPGs (Jurgens and Hage 2007). Vocal CPGs in many vertebrate species, including humans (i.e., a nonverbal vocal utterance, such as laughter), are considered to be located within the brain stem and thought to retain significant homology across species (Bass et al. 2008). The CPG underlying vocalizations in African clawed frogs (*Xenopus laevis*) presents an excellent model to understand the function of vocal CPGs.

Advertisement calls produced by male *X. laevis* to attract females consist of fast and slow trills, each of which contains a series of sound pulses that are repeated at ~60 and ~30 Hz, respectively (Fig. 1A). These calls are produced when laryngeal motoneurons fire at 60 and 30 Hz (Yamaguchi and Kelley 2000), causing contraction of a pair of laryngeal muscles at that rate that pull apart arytenoid discs to produce each sound pulse (Yager 1992). It is critical that the left and right laryngeal muscles are activated synchronously to generate a proper sound pulse. The central vocal pathways of *X. laevis* consist of two pairs of brain stem nuclei: n.IX-X, a homologue of nucleus ambiguus and retroambiguus (Albersheim-Carter et al. 2016) that contains laryngeal motoneurons projecting to the laryngeal muscles via the laryngeal nerve, and the premotor nucleus of the dorsal tegmental area of medulla (DTAM), a homologue of the parabrachial area (Fig. 1B) that does not include any lower motor or primary sensory neurons and thus is not associated with cranial nerves. Anatomical studies have shown that there are extensive reciprocal connections between these nuclei (Fig. 1B). In addition to these reciprocal connections within the

Address for reprint requests and other correspondence: A. Yamaguchi, Dept. of Biology, Univ. of Utah, 257 South 1400 East, Salt Lake City, UT 84112-0840 (e-mail: a.yamaguchi@utah.edu).

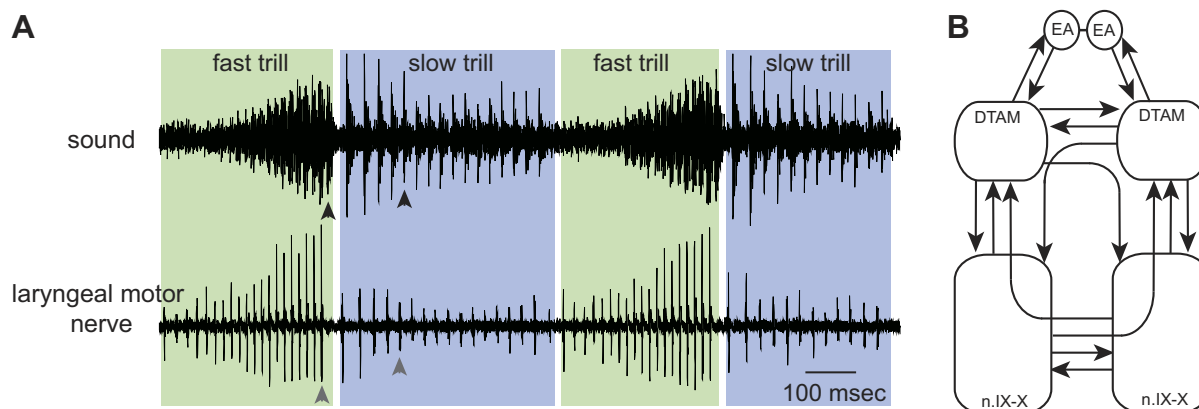


Fig. 1. Advertisement calls generated by male *Xenopus laevis*. *A*: simultaneous recordings of the sound (*top*) and the laryngeal nerve activity (*bottom*) while advertisement calls are produced by an awake male *X. laevis*. Fast trills are enveloped in green; slow trills in blue. A sound pulse (black arrowheads; *top*) is always preceded by a compound action potential (gray arrowheads; *bottom*). *B*: diagram of the key vocal nuclei of male *X. laevis*. Within a brain stem, a pair of dorsal tegmental area of medulla (DTAM) and a pair of laryngeal motor nuclei [a homologue of nucleus ambiguus (n.IX-X)] are contained. These nuclei are reciprocally connected with each other by projection neurons (arrows). DTAMs, in turn, are reciprocally connected with the extended amygdala (EA). A pair of EA is reciprocally connected, but the coupling is shown as a line in the diagram, since we did not explore the function of bilateral coupling of EA in this study.

brain stem, DTAM is reciprocally connected with the central amygdala (CeA) in the extended amygdala (Hall et al. 2013; Moreno and Gonzalez 2005) (Fig. 1*B*).

Previously, we developed a fictive vocalization preparation *in vitro* (Rhodes et al. 2007)—only one of a few fictive vocalizing preparations developed in vertebrates to date (Chagnaud et al. 2011). Application of serotonin (5-HT) to an isolated whole brain *in vitro* elicits fictive calls that can be recorded via laryngeal nerves. Here, with the use of the fictive calling preparation of male *X. laevis*, we analyzed the contribution of the projections connecting distinct brain stem nuclei to the rhythm generation, bilateral coordination, and initiation of calls. We discovered that CPGs for fast and slow trills include anatomically distinct populations of neurons contained in each lateral half of the brain stem whose timing is synchronized by the anterior and posterior commissures and that the initiation of fast trills appears to be mediated by a bilaterally synchronous signal provided by the extended amygdala to DTAM. Our results represent the first detailed analyses of these vocal CPGs and reveal new details of the functional architecture that underlies vocal production in male *X. laevis*, highlighting the complementary nature of the neural circuits that ensure bilateral synchrony in rhythm generation and subsequent call initiation.

MATERIALS AND METHODS

Animals

Forty-four adult male *X. laevis*, obtained from Nasco (Fort Atkinson, WI; average \pm SD weight = 42.98 ± 4.11 g, length = 7.16 ± 0.35 cm) were used for unilateral transverse transection (Fig. 2*A*; $n = 8$), anterior and posterior commissures sagittal transection (Fig. 3*A*; $n = 3$), anterior commissure sagittal transection (Fig. 4*A*; $n = 6$), posterior commissure sagittal transection (Fig. 5*A*; $n = 5$), descending inputs transverse and anterior commissure sagittal transection (Fig. 6*A*; $n = 4$), and descending inputs transverse transection (Fig. 7*C*; $n = 6$). All procedures were approved by the Institutional Animal Care and Use Committee at the University of Utah and complied with National Institutes of Health guidelines.

Isolated Brain Preparation and Fictive Vocal Recordings

Fictive vocalizations were elicited from the isolated brains of sexually mature adult males. Animals were anesthetized with subcutaneous injection (0.3 ml, 1.3%) of tricaine methanesulfonate (MS-222; Sigma, St. Louis, MO) and decapitated on ice, and brains were removed from the skulls in a dish containing cold saline (in mM: 96 NaCl, 20 NaHCO₃, 2 CaCl₂, 2 KCl, 0.5 MgCl₂, 10 HEPES, and 11 glucose, pH 7.8), oxygenated with 99% O₂. Brains were then brought back to room temperature (22°C) over the next hour and then transferred to a recording chamber that was superfused with oxygenated saline at 100 ml/h at room temperature.

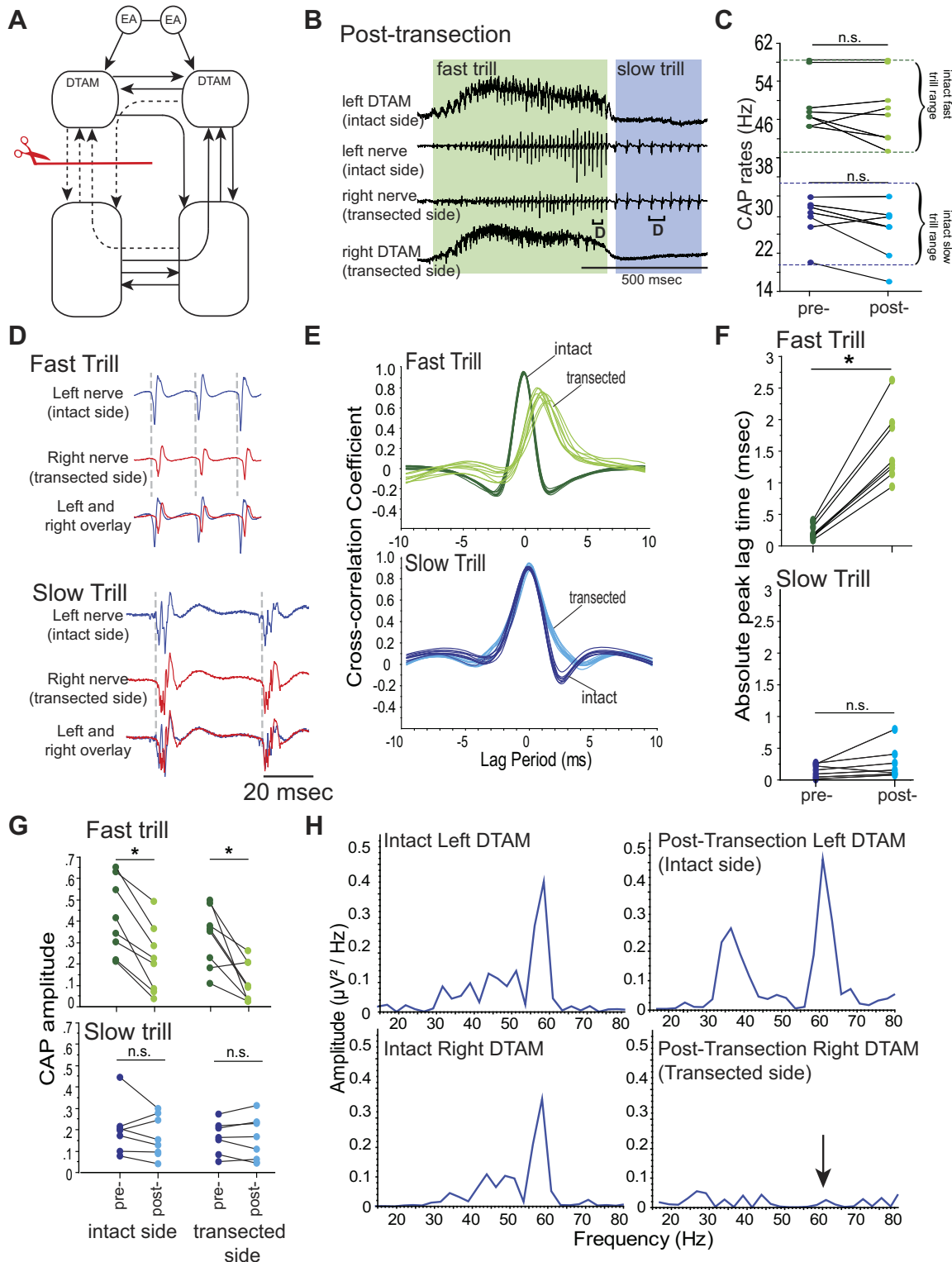
In these isolated brains, the laryngeal nerves are cut to ~ 7 mm in length to be used for nerve recordings. Laryngeal nerve activity was recorded bilaterally using a suction electrode placed over the cranial nerve IX-X. Local field potential (LFP) recordings from DTAM were obtained bilaterally using a 1-M Ω tungsten electrode (FHC, Bowdoin, ME). Fictive vocalizations were elicited by bath application of 5-HT (Sigma) using a 1-ml pipette. In response to 5-HT, a series of compound action potentials (CAPs) that are virtually identical to those recorded from awake calling frogs can be recorded from the laryngeal nerves of an isolated brain (Rhodes et al. 2007) (compare nerve recordings of Fig. 1*A* with 3*B*, for example). Before the application of 5-HT, superfusion of saline through the recording chamber was suspended, and 1 ml concentrated 5-HT solution (0.6 mM in dH₂O) was added to the 20-ml bath (30 μ M, final concentration). Nerve and LFP signals were amplified 1,000 \times using differential amplifiers (Models 1700 and 1800, respectively; A-M Systems, Carlsborg, WA) and were band-pass filtered (10–5 and 0.1–5 kHz, respectively). All signals were digitized at 10 kHz (Digidata 1440A; Molecular Devices, Sunnyvale, CA) and recorded on a personal computer using Clampex software (Molecular Devices). After 5 min of recording in the presence of 5-HT, superfusion was reinstated at the maximum rate (~ 10 ml/min) for 5 min to wash out the 5-HT and then at a slower rate (~ 125 ml/h) for 1 h between 5-HT applications.

Transection of Isolated Brains

After fictive advertisement calls were recorded from intact brains, transections were made using a scalpel. Before transection, brains were placed on ice and brought to $4 \pm 2^\circ\text{C}$. For unilateral transverse transection, a cut was made posterior to nerve VIII from midline to the lateral edge of the brain on either the left or right side of the brain stem (Fig. 2*A*). For anterior commissure sagittal transection, a cut was

made along the midline between the rostral optic tectum and cranial nerve V ventral to the ventricle (Fig. 4A), severing all of the projections between the two DTAMs. For posterior commissure sagittal transection, a cut was made along the midline between an area 1 mm rostral to the nerve IX-X and the obex ventral to the ventricle (Fig. 5A), severing all of the projections between the two n.IX-Xs. For descending inputs transverse transection, a cut was made at the level of the anterior optic tectum (Fig. 7C), severing all of the

connections between extended amygdala and DTAM. In brains with anterior and posterior commissure sagittal transection and those with anterior commissure sagittal and descending inputs transverse transection, both cuts were made in each brain (Figs. 3A and 6A, respectively). After the transection, the brains were placed in a holding dish containing oxygenated saline (200 ml) and gradually returned to room temperature over the next hour before 5-HT was applied again.



Analysis of *in Vitro* Fictive Vocalizations

To determine how transections affect the central vocal pathways, we examined the fictive fast and slow trill rates and the bilateral synchrony of the motor outputs produced. Ten bouts of calling were selected at random for each animal before and after the transection. CAPs corresponding to laryngeal motoneuron activity were identified using Clampfit (Molecular Devices), performing a threshold search function (threshold set at 3 SD of background noise, minimum event duration of 0.4 ms), and instantaneous CAP rates were calculated based on inter-CAP peak interval. When a brain produces a series of fictive advertisement calls, it is sometimes difficult to distinguish the end of fictive slow trills and the beginning of the next fictive fast trill. In this case, we used DTAM activity to distinguish the two types of fictive trills; CAPs accompanied by activity (or larger activity) in DTAM were defined as a part of fictive fast trills, and those without (or with smaller) DTAM activity were considered to be a part of fictive slow trills (see Fig. 3*B*, showing transition from slow to fast trills, for example). A frequency histogram of CAP rate during fictive fast and slow trills of each animal before and after transection showed a normal distribution and was fit with Gaussian curves with mean for fictive fast and slow trills, which was used for statistical analyses.

The *Xenopus* larynx generates sound pulses when both laryngeal muscles are activated simultaneously and pulls apart a pair of arytenoid discs. Accordingly, the central vocal pathways of intact *Xenopus* brains activate left and right laryngeal motoneurons nearly synchronously (see Fig. 3*C*, for example). To evaluate the synchronicity of the motor activity of the left and right side before and after the transection, cross-correlation coefficients between the left and right nerve activity were calculated while sliding one nerve recording against the other across time (± 10 ms; e.g., Fig. 3*F*). To this end, left and right nerve recordings containing 10 consecutive fictive fast and slow trill CAPs were used to calculate cross-correlation coefficients. The time of the maximum cross-correlation coefficients ("the peak lag time") was identified for fictive fast and slow trills before and after the transection for each animal. The peak lag time of zero indicates synchronous activity of the two nerves, and deviation from zero indicates delay between the two nerves. We took the absolute value of the peak lag time ("absolute peak lag time") for statistical tests, since our goal in most analyses was to determine how much the peak deviated from zero. In cases where we suspected that CAPs on one nerve lead the other, we also took the absolute value of the peak lag time to demonstrate the time lag between the two nerves. For the double transection that involves transection between extended amygdala and DTAM and anterior commissure (Fig. 6*A*), each CAP (instead of 10 consecutive CAPs) was cross correlated against the other to characterize moment-to-moment changes in the relative timing of CAPs on each side (Fig. 6).

Statistical Analyses

All statistical analyses were done using StatView software (SAS Institute, Cary, NC). For fictive trill rates, absolute peak lag time, and

maximum CAP amplitude for fictive fast and slow trills, Wilcoxon signed-rank test was used to compare the value before and after the transection within individuals.

RESULTS

Are Fast and Slow Trills Generated by the Same Neural Elements?

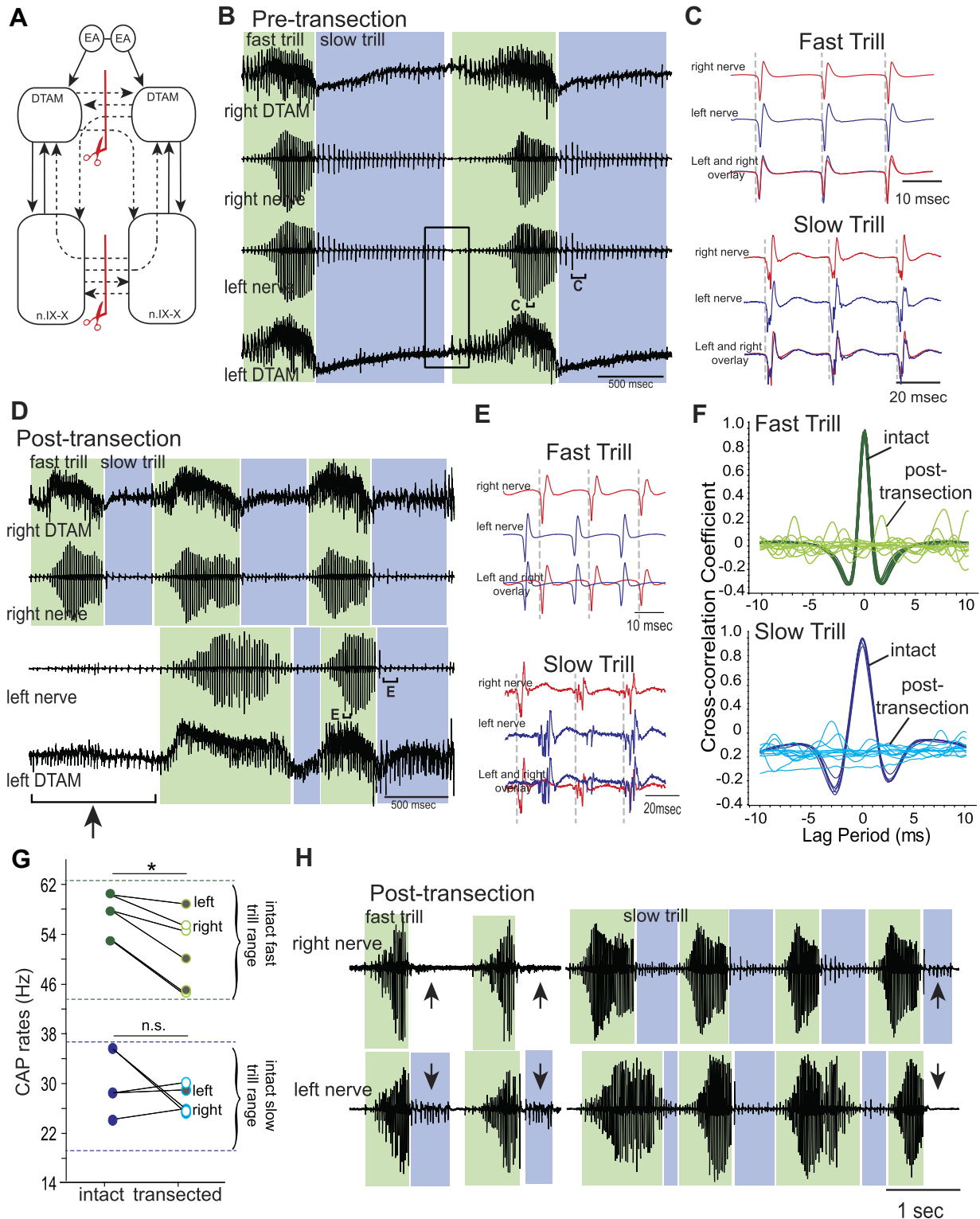
Are the fast and slow trills generated by shared neural circuitry or by anatomically distinct neural networks? Our previous study shows that LFP recordings obtained from DTAM are active mostly during fast but not during slow trills (see Figs. 3*B* and 7*A*, for example), suggesting that fast trills but not slow trills are mediated by DTAM. To test this possibility directly, we transected the projections between DTAM and n.IX-X (Fig. 2*A*) and examined the fictive advertisement calls elicited in response to 5-HT. Previously, we have shown that bilateral transection of the projection between the DTAM and n.IX-X transversely abolishes 5-HT-induced fictive call production entirely (Rhodes et al. 2007). With the absence of fictive vocalizations, however, it was not possible to determine if the transection disrupts the mechanisms underlying vocal initiation or the rhythm generation. Here, we reasoned that unilateral transection of the projection between n.IX-X and DTAM (unilateral transverse transection; Fig. 2*A*) may spare the vocal initiation and provide us with an opportunity to examine the role of the n.IX-X-to-DTAM projection in fast and slow trill generation.

In striking contrast to the bilateral transverse transection, the unilaterally transected brains produced fictive advertisement calls in response to 5-HT (Fig. 2*B*; $n = 8$). The rates of fictive fast and slow trill did not show any significant change after transection ($Z = -0.980, -1.694, P = 0.327, 0.091$ for fictive fast and slow trills, respectively; Fig. 2*C*), indicating that CPGs remaining in the transected brains are capable of generating normal vocal rhythms. However, fictive advertisement calls produced by the unilaterally transected brains showed some abnormality that was detected only during fictive fast trills. The timing of the CAPs recorded from the transected side significantly lagged behind those recorded from the intact side during fictive fast trills but not during fictive slow trills (Fig. 2*D*). Accordingly, the cross-correlation peak for fictive fast trills was not centered near zero after the transection, whereas the peak for the fictive slow trill remained near zero (Fig. 2*E*). Absolute peak lag time showed a significant increase only for fictive fast trills after the transection ($Z = -2.380, -1.690, P = 0.0172, 0.091$ for fictive fast and slow trills, respectively; Fig. 2*F*). In addition, the maximum amplitude of the CAPs

Fig. 2. Effects of unilateral, transverse transection of projections between DTAM and n.IX-X. *A*: diagram of the vocal pathways with transection marked with a red line with scissors, disconnected projections in dotted arrows, and intact projections in solid arrows. *B*: DTAM local field potential (LFP; *top* and *bottom*) and laryngeal nerve recordings (*middle 2*) obtained from right and left DTAMs and nerves while a fictive advertisement call is generated by an isolated brain before transection. Green and blue frames indicate fast and slow trills, respectively. Brackets with D are enlarged in *D*. *C*: fast and slow trill rates before and after transection. Each pair of points indicates mean fast and slow trill rates before and after the transection in 1 animal. Pairs of dotted green and blue lines indicate the range of fast and slow trill rates, respectively, obtained from intact brains. n.s., not significant; CAP, compound action potential. *D*: enlarged sections of brackets labeled in *B*. Left (blue) and right (red) nerve recordings are shown during fast and slow trills with the overlay of the 2 nerves at the *bottom*. *E*: example of cross-correlation between left and right nerve recordings (see MATERIALS AND METHODS) for fast and slow trills before and after transection. Each line represents cross-correlation of a bout of fast or slow trills from 1 animal (cross-correlation of 10 bouts shown). *F*: absolute peak lag time before and after the transection for fast and slow trills, plotted for each animal as in *C*. *G*: mean CAP amplitude during fast and slow trills obtained from brains before and after the transection. Each pair of points indicates mean fast and slow trill CAP amplitude before and after the transection in 1 animal. * $P < 0.05$, significant difference. *H*: example of the power spectra of the DTAM LFP recordings during fast trills from both sides of DTAM before and after transection. Arrow indicates the loss of peak at 60 Hz after the transection.

recorded from both of the nerves became significantly smaller after transection during fictive fast trills ($Z = -2.521, -2.380, P = 0.012, 0.017$ for intact and transected sides, respectively; Fig. 2G) but not during fictive slow trills ($Z = -0.676, -0.169, P = 0.499, 0.866$ for intact and transected sides, respectively; Fig. 2G). These results suggest that unilateral transection of the projection between n.IX-X and DTAM selectively impacts fast trills.

We suspected that the fast trill CPGs on the transected side became dysfunctional after transection, and the reason why the laryngeal motoneurons on the transected side generate any CAPs at all during fictive fast trills was because they were driven by the functional CPG on the contralateral intact side. To test this possibility, we examined LFP recordings obtained from the left and right DTAMs of the transected brains. As described previously (Zornik et al. 2010), DTAM LFP record-



ings of intact brains contain “waves” (baseline fluctuations) that coincide with onset and offset of the fictive fast trills and phasic activity riding on top of the waves (see Fig. 3*B*, for example) that peak at ~ 60 Hz (see Fig. 2*H*). In these transected brains, the LFP recordings obtained from DTAM on the intact side after the transection were no different than those obtained from intact brains, containing waves with phasic activity (see Fig. 2*B*) with a peak frequency ~ 60 Hz (Fig. 2*H*; compare before and after the transection). However, LFPs obtained from the transected side showed waves without phasic activity (Fig. 2*B*), as is evident in the loss of a peak in the power spectrum after the transection (Fig. 2*H*; compare before and after the transection). The LFP activity on the transected side resembles 5-HT-induced activity obtained from DTAM of brains in which DTAM and n.IX-X are bilaterally transected (Zornik et al. 2010). The results indicate that in the absence of the unilateral projections between DTAM and n.IX-X, the premotor activity in DTAM associated with fictive fast trills loses its phasic component and fails to drive the laryngeal motoneurons on the ipsilateral side, even though an indirect path from DTAM to ipsilateral n.IX-X (from DTAM to contralateral DTAM, contralateral n.IX-X to ipsilateral n.IX-X) is available. The laryngeal motoneurons on the transected side, instead, are likely driven by the fast trill CPG on the contralateral (intact) side. The fast trill inputs from the contralateral side to the transected side, however, appear insufficient to make up for the loss of excitatory drive from ipsilateral DTAM, which is known to provide direct, monosynaptic, glutamatergic inputs to the motoneurons (Zornik 2007). Based on these results, we conclude that the CPGs for fast and slow trills rely on anatomically distinct neuronal elements: the slow trill rhythm generator operates without the rostrocaudal projections between DTAM and n.IX-X, whereas the fast trill rhythm generator critically relies on these projections.

Are Commissural Interneurons Important for Rhythm Generation?

Many CPGs rely on a half-center oscillator that consists of two neurons (or two groups of neurons) that are reciprocally coupled to each other by inhibitory synapses (Moult et al. 2013; Sakurai et al. 2014; Satterlie 1985). Although the constituent neurons of the half-center oscillator are not rhythmogenic themselves, the reciprocal coupling together with the cellular mechanisms (such as escape from inhibition by activating hyperpolarization-activated cationic current or release of inhibition due to synaptic depression) endows the neurons with the ability to fire rhythmically at a variety of phases,

including anti-phase and in-phase, depending on the synaptic rise time (Van Vreeswijk et al. 1994; Wang and Rinzel 1992, 1993). Here, we examined whether anterior and/or posterior commissural interneurons in the *Xenopus* brain stem are a part of the reciprocal inhibitory network and constitute the core of the fast and/or slow rhythm generators. To test these possibilities, we transected anterior and posterior commissures in the sagittal plane (Fig. 3*A*) and examined the fictive advertisement calls generated by the transected brains in response to 5-HT application. If the commissures are a part of the half-center oscillator, then the transection of the anterior and/or posterior commissures should eliminate rhythmic activity.

When both anterior and posterior commissures of brains that generate fictive advertisement calls (Fig. 3*B*) were transected (Fig. 3*A*), fictive advertisement calls were still elicited in response to 5-HT (Fig. 3, *D* and *H*; $n = 3$). However, the fictive calls recorded from the right and left nerves became asynchronous after transection (Fig. 3, *D* and *E*). In intact brains, fictive fast and slow trills are initiated simultaneously (Fig. 3*B*), and the CAPs are synchronous, both during fictive fast and slow trills (Fig. 3*C*). Accordingly, the mean absolute peak lag time (see MATERIALS AND METHODS) between the CAPs recorded from the two laryngeal nerves of the intact brains was very small: 0.20 ± 0.03 and 0.27 ± 0.05 ms for fictive fast and slow trills, respectively (Fig. 3*F*). In the double-transected brains, in contrast, the onset and offset of the fictive fast and slow trills were not synchronous (Fig. 3*D* compared with *B*, but see below), with fictive calls and trills sometimes recorded only from one nerve and not from the other (Fig. 3*D*, the first fictive advertisement call recorded on the right but not on the left nerve; Fig. 3*H*, the first two calls contained fictive slow trills only on the left nerve, and the last call contained fictive slow trills only on the right nerve). Furthermore, the CAPs, recorded from the two nerves during fictive fast and slow trills, were entirely asynchronous; the number of CAPs produced in a given amount of time was not the same between the two nerves, and the delay between the CAPs recorded from the two nerves varied greatly from one instance to another (Fig. 3*E*). As a consequence, there was no obvious peak in the cross-correlation between the two nerve CAPs (Fig. 3*F*; note that there should be a peak in the cross-correlation if the activity of one nerve lags behind that of the other nerve with a consistent delay), and the maximum cross-correlation coefficient was reduced from 0.94 and 0.85 for the fast and slow trills of intact brains to 0.18 and 0.10 for the fast and slow trills of transected brains, respectively. Due to the absence of a clear peak in the CAP cross-correlation, we were not able to obtain a mean

Fig. 3. Effects of sagittal transection of both anterior and posterior commissures on fictive vocalizations. *A*: diagram of the vocal pathways showing transections in red lines with scissors, transected projections in dotted arrows, and intact projections in solid arrows. *B*: example of the bilateral DTAM LFP recordings (*top* and *bottom*) and laryngeal nerve recordings (*middle 2*) obtained during fictive advertisement calls before transection. Green and blue frames indicate fast and slow trills, respectively, for all figures. Rectangle shows transition from slow trills to fast trills. Brackets with C are enlarged in *C*. *C*: enlarged sections of brackets labeled in *B*. Left (blue) and right (red) nerve recordings are shown during fast and slow trills with the overlay of nerve activities at the *bottom*. *D*: example of the bilateral DTAM LFP and laryngeal nerve recordings obtained from a brain in which both anterior and posterior commissures are sagittally transected. Bracket with arrow points to a fictive advertisement call produced only by the right nerve. Brackets with E are enlarged in *E*. *E*: enlarged sections from small brackets labeled in *D*. *F*: example of cross-correlation between left and right nerve recordings for fast and slow trills before (intact) and after (post-transection) transection. There is no obvious peak in correlation coefficient after the transection, indicating the asynchronous nature of the 2 nerve activities. *G*: mean fast and slow trill rates before and after transection from 3 brains. Because asynchronous fictive calls were recorded from the right and left nerve, the trill rates from the 2 sides were analyzed as independent rhythms after transection. Points connected by a line indicate mean fast and slow rate of 1 animal. Pairs of dotted green and blue lines indicate the range of fast and slow trill rates, respectively, obtained from intact brains. * $P < 0.05$, significant difference. *H*: example of fictive advertisement calls recorded from the right and left laryngeal nerves from brains with both anterior and posterior commissures sagittally transected. Note that the left and right calls are largely overlapping, but slow trills are sometimes missing on 1 nerve (arrows).

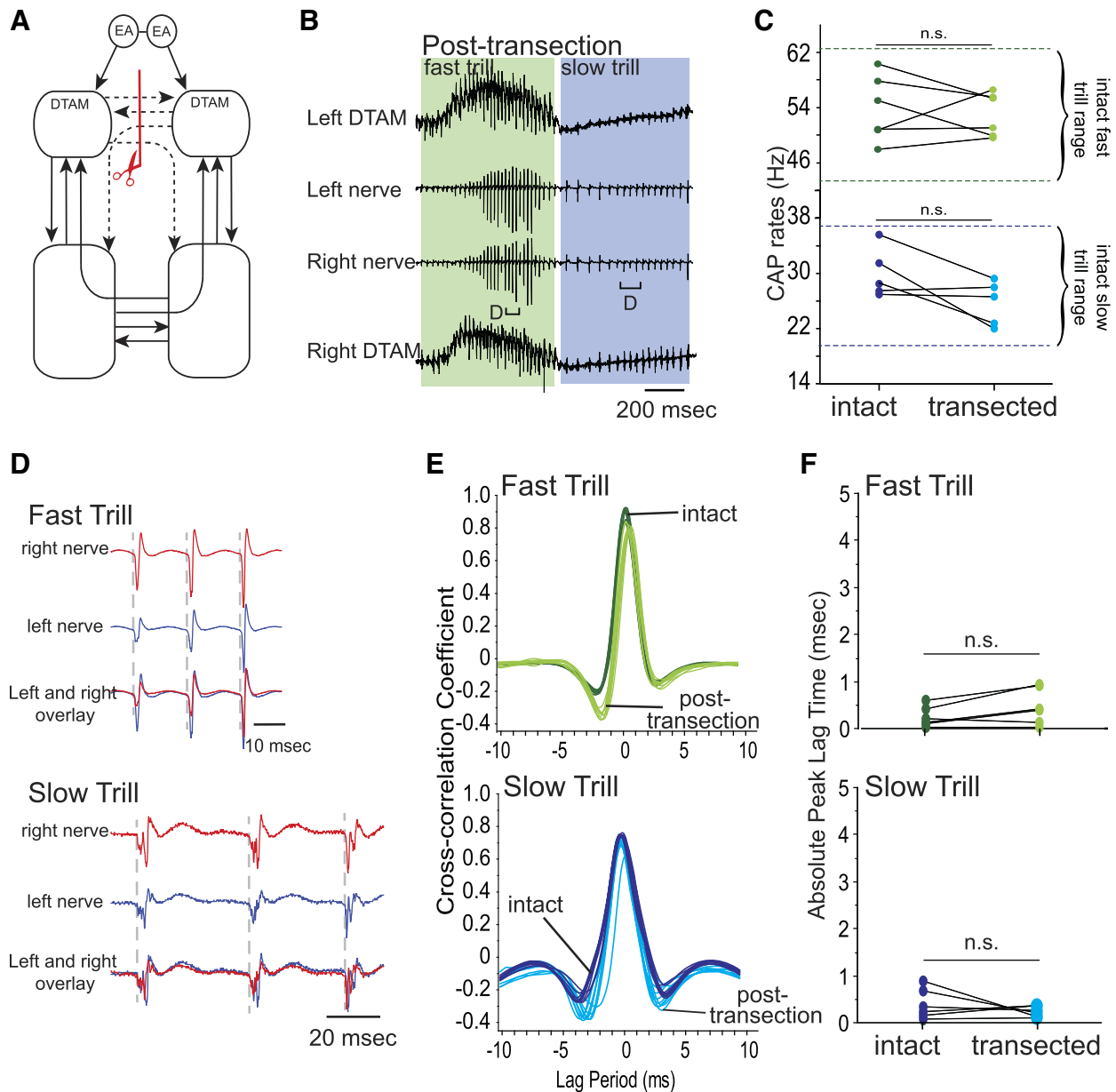


Fig. 4. Effects of sagittally transecting anterior commissure alone on fictive advertisement calls. *A*: diagram of the vocal pathways showing the transection in red line with scissors, transected projections in dotted arrows, and intact projections in solid arrows. *B*: example of the bilateral DTAM LFP (*top* and *bottom*) and laryngeal nerve recordings (*middle 2*) obtained during a fictive advertisement call from a brain after anterior commissure sagittal transection. Green and blue frames indicate fast and slow trills, respectively. Brackets with *D* are enlarged in *D*. *C*: mean fast and slow trill rates before and after transection from 6 brains. Points connected by a line indicate mean fast and slow rate of 1 animal. Pairs of dotted green and blue lines indicate the range of fast and slow trill rates, respectively, obtained from intact brains. *D*: enlarged sections of brackets labeled in *B*. Left (blue) and right (red) nerve recordings are shown during fast and slow trills with the overlay of the 2 nerve activity at the *bottom*. *E*: example of cross-correlation between the left and right nerve recordings for fast and slow trills before and after transection. *F*: absolute peak lag time before and after transection, plotted for each animal as in *C*.

absolute peak lag time from these transected brains. These results are consistent with the idea that the commissures are not necessary for rhythm generation but that they function to synchronize the motor outputs from the two nerves.

Next, to examine the capability of rhythm generation of the fast and slow trill CPGs in the left and right brain stem in isolation, we analyzed the rates of the fictive fast and slow trills produced by double-transected brains. Since the two sides of the brain produce independent vocal motor programs, we analyzed the fictive fast and slow trill rates recorded from each nerve separately. The results showed that after double transec-

tion, fictive fast trill rates recorded from the two nerves decreased ($Z = -2.201$, $P = 0.028$), whereas fictive slow trill rates remain unchanged ($Z = -0.405$, $P = 0.686$; Fig. 3*G*). Although the decrease of the fast trill rates was statistically significant, fictive fast trill rates after transection remained within the normal range of fast trills generated by intact brains (Fig. 3*G*). Thus CPGs, contained in the right and left halves of the brain stem, are capable of generating basic fast and slow trill rhythms.

To explore the function of the isolated hemibrain stem further, we examined premotor activity obtained from the

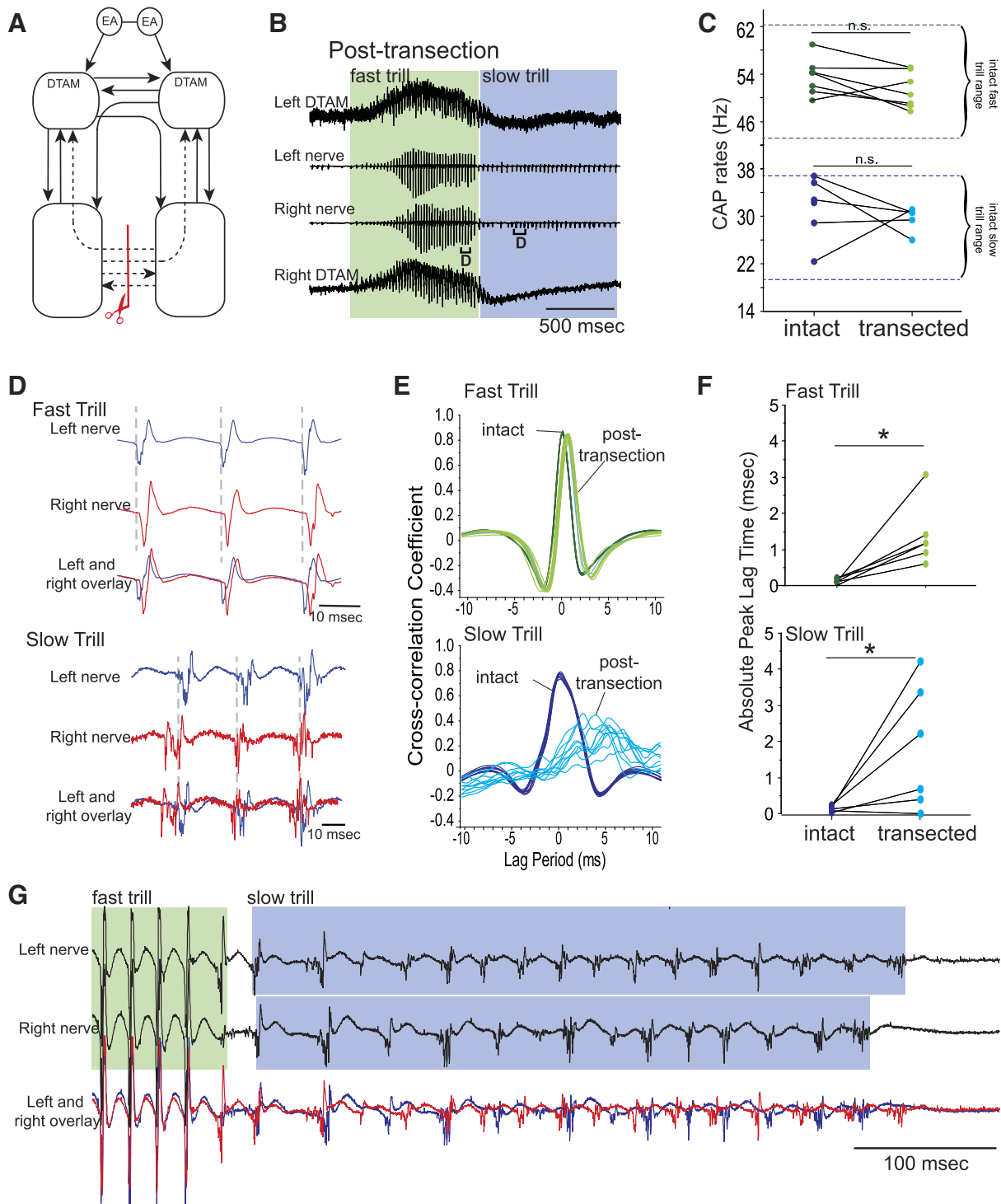
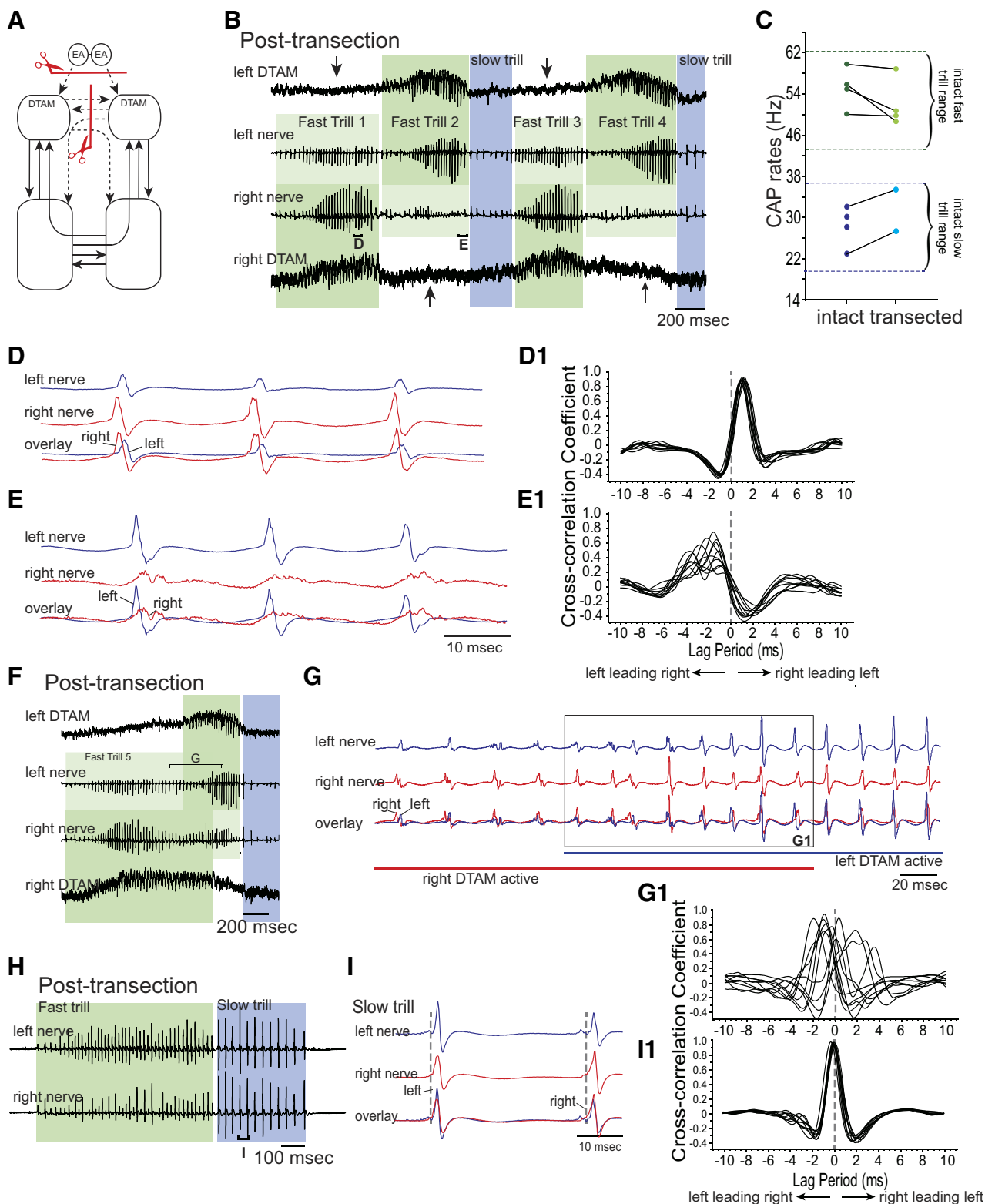


Fig. 5. Effects of sagittally transecting the posterior commissure alone on fictive advertisement calls. *A*: diagram of the vocal pathways showing the transection in red line with scissors, transected projections in dotted arrows, and intact projections in solid arrows. *B*: example of the bilateral DTAM LFP (*top* and *bottom*) and laryngeal nerve recordings (*middle 2*) obtained during fictive advertisement call after posterior commissure sagittal transection. Green and blue frames indicate fast and slow trills, respectively, for all figures. Brackets with D are enlarged in *D*. *C*: mean fast and slow trill rates before and after transection from 6 brains. Each pair of points indicates mean rate before and after transection in 1 animal. Pairs of dotted green and blue lines indicate the range of fast and slow trill rates obtained from intact brains. *D*: enlarged sections of brackets labeled in *B*. Left (blue) and right (red) nerve recordings are shown during fast and slow trills with the overlay of the nerve activities at the *bottom*. *E*: example of cross-correlation between the left and right nerve recordings for fast and slow trills before and after transection. *F*: absolute peak lag time before and after the transection, plotted for each animal as in *C*. * $P < 0.05$, significant differences. *G*: example of the left and right nerve recordings during a fictive fast and slow trill. In this recording, left and right CAPs are largely asynchronous only during the slow trill.

DTAMs of double-transected brains. These recordings showed activity-containing waves and phasic activity, as in intact brains, but the activity accompanied the fictive fast trill recorded from the ipsilateral, not from the contralateral, nerve (Fig. 3D), confirming that each side of the brain stem generates its own fictive fast trill rhythms independently. Thus DTAM is capable of generating normal premotor activity in the absence

of the two commissures. Together, these results suggest the following: 1) that the left and right brain stem contains autonomous CPGs for fast and slow trills that can generate basic vocal rhythms even when they are surgically isolated from their contralateral counterparts and 2) that the commissures function to synchronize bilaterally the activity of the CPGs on the two sides of the brain stem.



Which Commissures Are Important for Bilateral Coordination?

We next examined which of the commissures play a role in synchronizing the two separate CPGs on each side of the brain stem. To this end, we first transected the anterior commissure alone (Fig. 4A). These transected brains readily produced fictive fast and slow trills (Fig. 4B; $n = 6$), and both trill rates did not change significantly after transection ($Z = -0.314$, -1.572 , $P = 0.753$, 0.116 for fictive fast and slow trills, respectively; Fig. 4C). In addition, the CAPs recorded from the two nerves appeared synchronous (Fig. 4, D and E), and accordingly, the absolute peak lag time showed little change for fictive fast and slow trills ($Z = -0.943$, -0.943 , $P = 0.345$, 0.345 for fictive fast and slow trills, respectively; Fig. 4F). Thus the anterior commissure by itself is not necessary for synchronizing the timing of CAPs generated by the right and left CPGs. Instead, the projections remaining in the brain stem (see Fig. 4A) can synchronize the timing of fast and slow trill CAPs generated by the two sides of the brain stem.

When the posterior commissure was transected alone (Fig. 5A), fictive fast and slow trills were readily produced in response to 5-HT (Fig. 5B; $n = 5$), and fictive fast and slow trill rates did not change significantly after transection ($Z = -1.352$, -0.674 , $P = 0.176$, 0.5 for fictive fast and slow trills, respectively; Fig. 5C). The timing of CAPs recorded from the right and left sides, however, became less synchronous after transection during both fictive fast and slow trills (Fig. 5, D and E). The absolute peak lag time between the right and left CAPs increased, on average (\pm SE), by 1.27 ± 0.36 and 2.01 ± 0.72 ms during fictive fast and slow trills, respectively, and these increases were significant ($Z = -2.201$, -2.023 , $P = 0.028$, 0.043 for fictive fast and slow trills, respectively; Fig. 5F). These results suggest that the posterior commissure plays a role in coupling the CPGs contained in the left and right brain stem. Some or all of the projection neurons that were eliminated in these brains (see Fig. 5A) contribute to bilaterally synchronizing the CAPs, and the remaining projections (see Fig. 5A) are not sufficient to compensate for the loss.

Although the majority of the fictive slow trills recorded from the brains with transected posterior commissures consists of CAPs with a consistent delay between the two nerves, as described above (Fig. 5D), some fictive slow trills recorded from the right and left nerves of the transected brains appeared

asynchronous. An example in Fig. 5G shows fictive slow trills recorded from the right and left nerves of a brain with the posterior commissure transected. The fictive slow trill recorded from the two nerves contained different numbers of CAPs (16 CAPs on the left nerve; 14 CAPs on the right nerve) that were repeated at rates that differ between the two nerves. This asynchrony between the two nerves was never observed during fictive fast trills, indicating that the posterior commissure plays a more important role for the bilateral synchronization of the slow trill CPG than that of the fast trill CPG. Taken together, neither of the single transections completely and consistently decoupled the CPGs on the two halves of the brain stem, indicating that the two commissures play complementary roles in bilaterally synchronizing the CPGs.

Do Descending Projections from Extended Amygdala to DTAM Initiate Fast Trills from the Two Sides of the Brain Stem Synchronously?

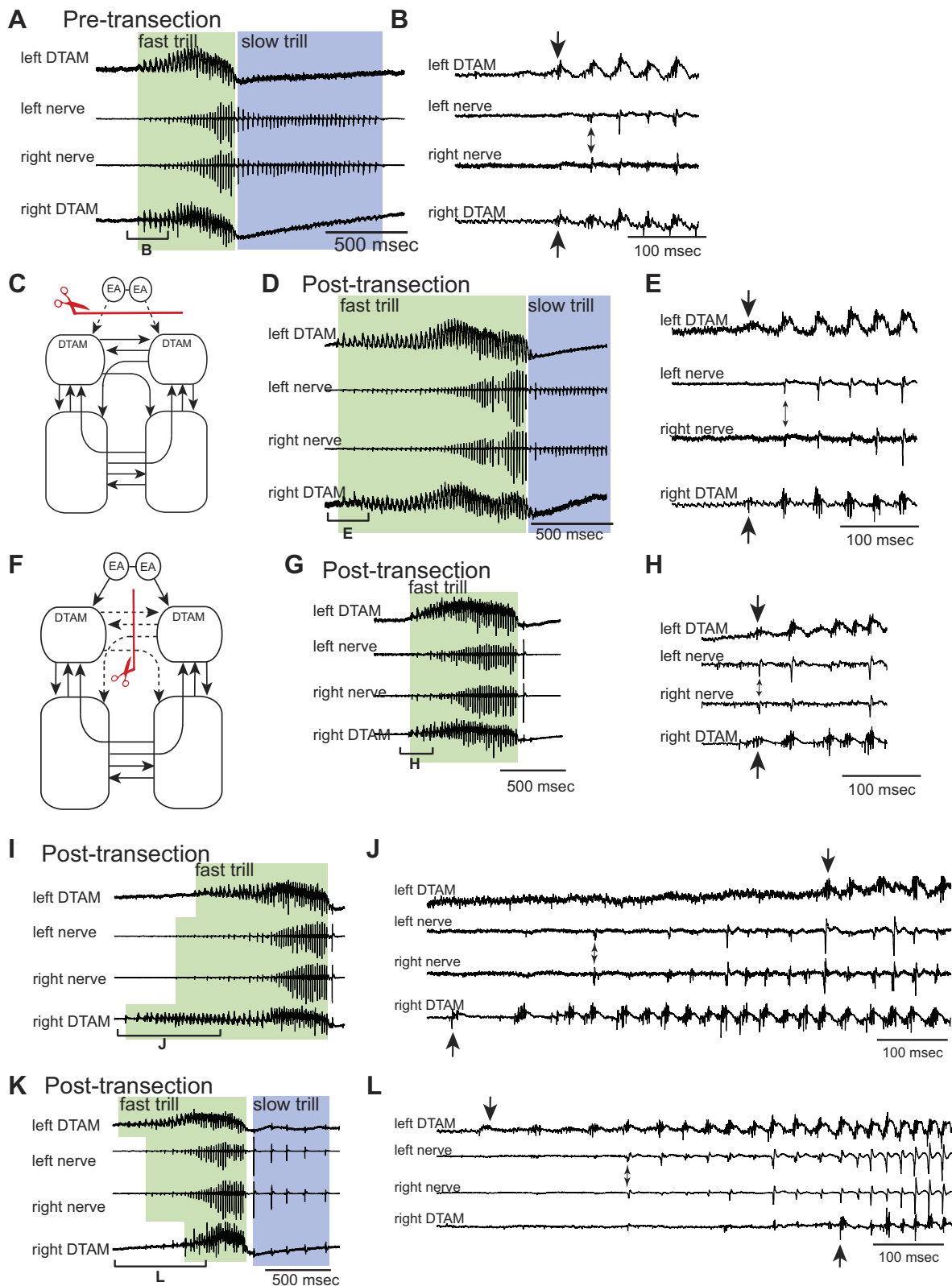
In *X. laevis*, the bed nucleus of the stria terminalis (BNST) has been shown to be involved in male vocalizations. BNST is known to project to the rostral raphe nucleus (Moreno et al. 2012), which expresses 5-HT_{2C} receptors that mediate initiation of fictive advertisement calls (Yu and Yamaguchi 2010). Electrical stimulation of the BNST in vitro elicits fictive advertisement calls, and the lesioning of BNST in vivo reduces the calling behavior (Hall et al. 2013). Previously, however, we showed that a brain stem isolated from the descending inputs by transversely transecting at the level of the rostral optic tectum can still produce fictive advertisement calls in response to 5-HT (Rhodes et al. 2007), suggesting that extended amygdala is not necessary for the initiation of the advertisement calls. To resolve this paradox, we explored the mechanisms underlying initiation of fictive fast trills.

Analyses of the fictive advertisement calls produced by the brains with sagittal transections of anterior and posterior commissures provided evidence that descending projections from the extended amygdala to DTAM may play a role in initiating advertisement calls from the two sides of the brain stem simultaneously. In these double-transected brains, fictive calls were sometimes recorded only from one side and not from the other (Fig. 3D; the first call only recorded from the right nerve). However, the majority of the calls (93.8%) was initi-

Fig. 6. Effects of simultaneously eliminating the anterior commissure and the projection between the EA and DTAM on fast trill initiation. A: diagram of the vocal pathways showing the transection in red line with scissors, transected projections in dotted arrows, and intact projections in solid arrows. B: example of the bilateral DTAM LFP (top and bottom) and nerve recordings (middle 2) obtained from double-transected brains. Dark and light green frames indicate the side with the larger and smaller amplitude fast trill CAPs, respectively. Blue frames indicate slow trills. During fast trill 1 and 3, CAPs are larger on the right nerve than the left nerve, and during fast trill 2 and 4, CAPs are larger on the left nerve than the right nerve. Arrows indicate the unilateral absence of the DTAM activity. Brackets with D and E are enlarged in D and E. C: mean fast and slow trill rates before and after transection. Each pair of points indicates mean trill rates for 1 animal. Pairs of dotted green and blue lines indicate the range of fast and slow trill rates, respectively, obtained from intact brains. D and E: enlarged views of the brackets labeled in B. D1 and E1: example of cross-correlation between the left and right nerve shown in D and E. Here, the cross-correlation coefficient was calculated by a sliding recording of a single CAP obtained from 1 nerve against the other nerve (as opposed to using nerve recordings of whole fast trills, as done in previous figures). Peak cross-correlation coefficient at negative or positive lag time indicates left nerve leading right or right nerve leading left, respectively. F: example of the bilateral DTAM LFP (top and bottom) and laryngeal nerve recordings (middle 2) during which both left and right DTAM becomes active. Dark and light green frames indicate the side with larger and smaller amplitude fast trill CAPs, respectively, as in B. Blue frame indicates a slow trill. Bracket with G is enlarged in G. G: enlarged view of the bracket labeled in F. Left (blue) and right (red) nerve recordings are shown with the overlay of the nerve activities at the bottom. Blue and red straight lines under the traces indicate the time during which left and right DTAM is active, respectively. G1: example of cross-correlation between the left and right nerve. Note that the peak cross-correlation coefficients are distributed between positive and negative lag times, indicating that CAPs recorded from 1 nerve do not consistently lead those recorded from the other nerve. H: example of bilateral nerve recordings obtained from double-transected brains that include slow trills. Bracket with I is enlarged in I. I: enlarged view of the bracket labeled in H. I1: example of cross-correlation between the left and right nerves during slow trills. Note that peak cross-correlation coefficients are centered at 0, indicating that the CAPs recorded from the 2 nerves are synchronous.

ated from both sides within a relatively short time window; after a fictive fast trill is initiated by one side of the brain, the other side initiated the fictive fast trills within 7.0–316.4 ms in double-transected brains (average delay = 95.0 ms). Thus most calls recorded from the right and left nerves showed extensive

overlap with each other (e.g., Fig. 3H), even though CAPs are not at all synchronous (Fig. 3E). This observation suggests that in these double-transected brains, there is a bilaterally synchronous signal descending from the extended amygdala to right and left DTAM that allows the fictive fast trills to be initiated



by both sides of the brain stem near synchronously in response to 5-HT.

In another experiment, we fortuitously discovered that there are redundant mechanisms within the central vocal pathways of *X. laevis* to initiate synchronous fast trills from the left and right sides. In four brains, sagittal transection was made to sever the anterior commissure, and bilateral transverse transection was made at the level of rostral optic tectum to remove descending inputs from the external amygdala to DTAMs. Out of four double-transected brains, only two produced full fictive advertisement calls, including both fast and slow trills, and the remaining two produced calls that include only fast trills. Thus we focused on the initiation of fast trills using all four brains. In these double-transected brains, fictive fast trills were initiated from both nerves near simultaneously (see Fig. 6*B*). However, the amplitude and timing of the CAPs recorded from the two nerves were abnormal. In these brains, fictive fast trill CAPs recorded from one nerve had a significantly larger amplitude than those of their contralateral counterpart. Which nerve had a larger CAP amplitude was not consistent and often alternated. For example, in Fig. 6*B*, the CAP amplitude of the right nerve is larger than that of the left nerve during the first and third fictive fast trills and smaller during the second and fourth fictive fast trills (see Fig. 6*B*). Furthermore, when the timing of fictive fast trill CAPs recorded from the right and left nerves was examined, the side with the larger CAPs always preceded the side with the smaller CAP (Fig. 6, *D*, *DI*, *E*, and *EI*). These results suggest that premotor activity of the fictive fast trills is generated only by one side (right or left) of the brain stem in these double-transected brains and projects to the silent side to drive the motoneurons. To explore this possibility, we examined premotor activity in DTAM directly.

Strikingly, the LFP wave and phasic activity in DTAM were only observed when the ipsilateral nerve produced large-amplitude CAPs (Fig. 6*B*). DTAM was silent on the side producing the delayed, small-amplitude CAPs (Fig. 6*B*). This observation suggests that in these double-transected brains, fictive fast trills are initiated and generated entirely by DTAM on one side (left or right) of the brain stem, whereas the other side remains silent.

Moreover, we found that activity in the two DTAMs could overlap in time. For example, in Fig. 6*F*, right DTAM becomes active first and generates fictive fast trills with a large CAP amplitude that precedes the small CAPs recorded from the left nerve (Fig. 6, *F* and *G*). Approximately 800 ms later, the left DTAM becomes active, and the right DTAM continues to be active. This simultaneous activity of right and left DTAM results in CAPs from both nerves with variable amplitude and delay (Fig. 6, *G* and *GI*). After ~200 ms of simultaneous

DTAM activity, right DTAM becomes silent, and left DTAM continues its activity for another ~200 ms by itself while larger amplitude CAPs with a slight lead relative to the right CAPs are recorded from the left nerve (Fig. 6*G*). This observation suggests that in these double-transected brains, the fictive fast trill is initiated by each side independently without any temporal coordination between the two sides. Thus in these double-transected brains, we were able to initiate fast trills from either side of the brain stem independently.

Interestingly, in these transected brains, we observed that fictive slow trills were initiated simultaneously (Fig. 6*H*) and that CAPs recorded from the two nerves were synchronous (Fig. 6, *I* and *II*). These results indicate that even though the fictive fast trills are initiated autonomously by each side of the brain stem in these double-transected brains, initiation and generation of fictive slow trills are unaffected, suggesting that the mechanisms of trill initiation differ between the fast and slow trill CPGs.

The results obtained from the double-transected brains are in stark contrast to results obtained from the brains with either one of the transections alone. In brains in which the projection from extended amygdala to DTAM is transected (Fig. 7*C*; $n = 6$), fictive vocalizations are readily elicited in response to 5-HT (Fig. 7*D*), as we have described previously (Rhodes et al. 2007), and the premotor activity is also initiated simultaneously by the left and right DTAM (see Fig. 7*E*), as in the case of intact brains (see Fig. 7*B*). This premotor activity in intact and transected brains resulted in the simultaneous onset of fast trill CAPs from the two nerves (see Fig. 7, *B* and *E*). When the anterior commissure was transected, we found that the onset of premotor activity that accompanies fictive fast trills (Fig. 7, *G*, *I*, and *K*) was variable. Premotor activity of the two DTAMs was sometimes initiated simultaneously (see Fig. 7*H*), but at other times, the activity in one DTAM preceded the activity in the contralateral DTAM (see Fig. 7, *J* and *L*) by as long as 500 ms (e.g., Fig. 7*J*). Asynchronous initiation of DTAM activity is unlikely to be due to the positioning of the extracellular electrode, because these distinct patterns of DTAM activity (such as Fig. 7, *H*, *J*, and *L*) were observed in many consecutive calls when the electrodes were stationary. Despite the variability in the initiation of DTAM activity in these transected brains, the first CAP of the fictive fast trill appears to be generated from both nerves simultaneously (see Fig. 7, *H*, *J*, and *L*), presumably because the laryngeal motoneurons of the silent side are driven by the premotor signal from the contralateral active side. Taken together, the loss of one of the two projections does not cause unilateral fictive fast trill initiation, even though the transection of anterior commissure alone sometimes introduced the delay in the initiation of DTAM

Fig. 7. Effects of transecting the projection between EA and DTAM alone or the anterior commissure alone on the initiation of DTAM premotor activity and fast trills. *A*: example of the bilateral DTAM LFP (*top* and *bottom*) and nerve recordings (*middle 2*) obtained from an intact brain. Green and blue frames indicate fast and slow trills, respectively, for all figures. Bracket with *B* is enlarged in *B*. *B*: enlarged view of the bracket labeled in *A*. The first premotor activity recorded from left and right DTAM is labeled with the large arrows (*top* and *bottom*), and the first fast trill CAPs recorded from the left and right nerves are labeled with a small, double-headed arrow (*middle 2*). Note that both DTAM activity and CAPs are initiated simultaneously from the left and right. *C* and *F*: diagrams showing transection sites in red lines with scissors, transected projections in dotted arrows, and intact projections in solid arrows. *D*, *G*, *I*, and *K*: examples of the bilateral DTAM LFPs (*tops* and *bottoms*) and nerve recordings (*middle 2* of each) obtained after transection to eliminate the projections between EA and DTAM (*D*) or anterior commissure (*G*, *I*, and *K*). Brackets with *E*, *H*, *J*, and *L* are enlarged in *E*, *H*, *J*, and *L*, respectively. *E*, *H*, *J*, and *L*: enlarged view of the brackets labeled in *D*, *G*, *I*, and *K*, respectively. The first premotor activity recorded from left and right DTAMs is labeled with large arrows (*top* and *bottom*), and the first fast trill CAPs recorded from the left and right nerves are labeled with small, double-headed arrows (*middle 2* of each), as in *B*. Note that DTAM premotor activity starts simultaneously in *E* and *H* but not in *J* and *L*. The first fast trill CAPs, in contrast, are always recorded simultaneously from the 2 nerves in these transected brains.

activity. Thus we suggest that these two projections play redundant roles in initiating fast trills from the two sides simultaneously, and removal of both of the projections is required to decouple fast trill initiation from the two sides.

DISCUSSION

Our results reveal the basic architecture of the vocal CPG that regulates call rhythm generation, coordination, and initiation. Based on these results, we propose a model of the vocal pattern generator in male *X. laevis*, as discussed below (Fig. 8).

CPGs for Fast and Slow Trills

In this study, we first examined if neural elements that make up the fast and slow CPGs are distinct. A male *X. laevis* is known to change the duration of the fast and slow trills depending on its state of arousal; when a male detects a sexually receptive females, the duration of the fast trill is elongated, whereas the duration of slow trills is shortened. It is conceivable that the neural circuitry that generates the two trill types contains anatomically distinct populations of neurons and is regulated independently.

In a variety of animals, the generation of different patterns of motor behaviors using the same muscles is accomplished within the central nervous system in a number of different ways (such as biting and chewing). First, related motor patterns can be generated by anatomically distinct networks dedicated to each motor program (Huang and Satterlie 1990; Satterlie 2013). Second, they can be generated by networks that are reorganized to be multifunctional (Berkowitz 2010; Dickinson et al. 1990; Hooper and Moulins 1989, 1990; Li 2015; Meyrand et al. 1991, 1994; Popescu and Frost 2002; Weimann

and Marder 1994). A third strategy involves the combination of the two (Berkowitz 2010; Briggman and Kristan 2006). Our results indicate that the circuits for fast trill generators include a population of neurons in DTAM that are distinct from those involved in slow trill generation, although the two circuits may share neurons in the n.IX-X. When the projections between n.IX-X and DTAM are unilaterally transected in male *X. laevis*, fast trill premotor activity recorded from DTAM became abnormal, and the fast trill (CAPs) recorded from the transected side consistently lagged behind those recorded from the intact side, whereas the slow trill CAPs remained intact. These results are consistent with the idea that the transection destroyed the core element of the fast trill rhythm generator on the transected side, whereas the fast trill generator on the intact side and the slow trill generators on both sides remained intact. Thus we suggest that the fast trill CPG (see Fig. 8A) includes a dedicated population of neurons (projection neurons that span n.IX-X and DTAM; Fig. 8A) along with neurons in n.IX-X, whereas the slow trill CPG consists of neurons in the n.IX-X (see Fig. 8A). Whether neurons in n.IX-X are shared by the two circuits is yet to be determined, but these are shown as separate populations in Fig. 8A for simplicity.

Phylogenetically, males of the majority of the species in the genus *Xenopus* produce a series of sound pulses at rates similar to the fast trills of *X. laevis*, whereas others produce sound pulses at a rate similar to or slower than the slow trills (Evans et al. 2015; Leininger et al. 2015; Tobias et al. 2011). It will be of interest to examine if all of the species that generate fast trill-like calls use mechanisms that involve both nuclei, whereas the slow trill-like calls are generated entirely by n.IX-X. Recent studies suggest that at least in two species of *Xenopus* that generate fast trill-like calls, DTAM premotor

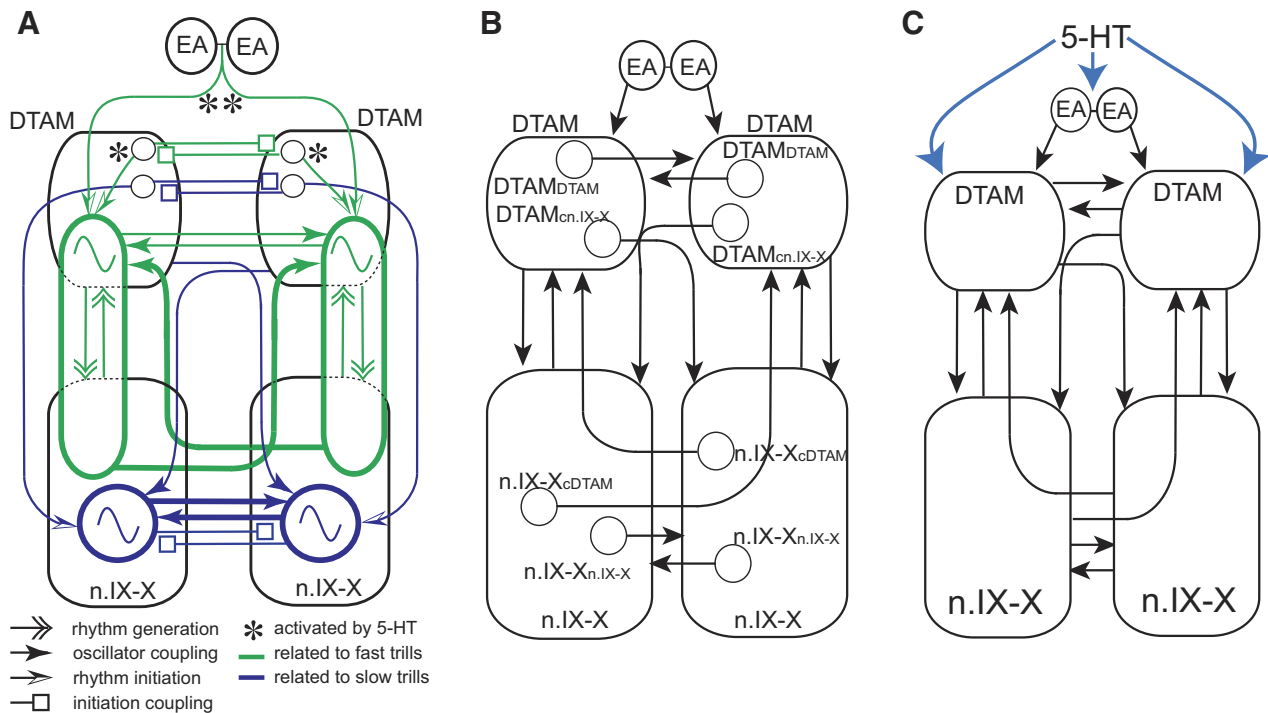


Fig. 8. Model of the vocal central pattern generators (CPGs) in male *X. laevis*. **A**: functional model of the central vocal pathways of male *X. laevis*. Green ovals and blue circles containing sinusoidal waveform indicate CPGs for fast and slow trills, respectively. **B**: four different types of anatomically identified projection neurons in the central vocal pathways of *X. laevis*. Axons of these neurons are contained in anterior or posterior commissures. **C**: blue arrows indicate hypothesized redundant mechanisms of vocal initiation by serotonin (5-HT).

activity similar to that recorded in *X. laevis* is obtained (C. L. Barkan, E. Zornik, and D. B. Kelley, personal communication), supporting at least a part of this hypothesis. Additionally, we previously found that administration of androgen to adult females masculinizes them to produce male-like advertisement calls (Potter et al. 2005). As the vocalizations masculinize, it is possible that new projections between DTAM and n.IX-X are formed to construct the fast trill CPG de novo.

Fast and Slow Trill CPGs Are Contained in the Two Lateral Hemispheres of the Brain Stem

A half-center hypothesis to explain mechanisms underlying rhythmic motor programs was originally proposed by Brown (1911, 1914) and has been examined both experimentally and computationally in a variety of species to date. Here, we asked whether the anterior and posterior commissures in the brain stem of *X. laevis* were components of a half-center oscillator and are necessary for the production of fast and slow trill rhythms. Transection of either one or both commissures did not result in the loss of fictive fast and slow trill rhythms, except for a slight decrease in the fictive fast trill rate, indicating that the commissures are not part of the half-center oscillators and that the basic components of the fast and slow trill rhythm generators are contained in the two lateral halves of the brain stem. Although the sound-pulse rates were largely unaffected, the vocalizations produced by the isolated hemibrain stems were no longer bilaterally synchronized in brains in which both commissures were transected, indicating that the commissures function to synchronize the fast and slow trill generators on each side. Similar results were obtained in the Northern leopard frog; a complete sagittal bisection of the brain stem in vitro did not abolish fictive vocalizations elicited in response to electrical stimulation delivered to the anterior optic area (Schmidt 1992). In locomotor CPGs, surgical separation of the two sides of the spinal cord or pharmacological blockade of inhibitory synapses (including reciprocal inhibition) failed to abolish unilateral rhythmic activity underlying locomotor programs in lampreys, tadpoles, and mice (Cangiano and Grillner 2003; Cangiano et al. 2012; Cohen and Harris-Warrick 1984; Cowley and Schmidt 1995; Hinckley et al. 2005; Kwan et al. 2009; Li et al. 2010), suggesting that the commissures in the spinal cord of these species are not necessary components of the rhythm-generating mechanisms. In contrast, locomotor CPGs of invertebrates have been shown to rely on half-center oscillators for rhythm generation (Sakurai et al. 2014; Satterlie 1985). Although these results seem to indicate that half-center oscillators play more dominant roles in invertebrates than in vertebrates, a recent study of a swimming CPG in *Xenopus* tadpoles showed that pharmacological blockade of reciprocal inhibition results in homeostatic change within the network that reinstates the rhythmic activity after tens of minutes (Moult et al. 2013). It is not clear how prevalent such homeostatic recovery is among different neural circuits, but it is possible that fictive fast and slow trill rhythms observed after >60 min of transection in this study may be due to de novo modification of the neural circuits to regain function, as in swimming circuits of *Xenopus* tadpoles. Future research that involves selective and fast inactivation of the commissural interneurons will be required to answer this question. At present, however, we tentatively conclude that there are fast

and slow trill CPGs in each side of the brain stem (Fig. 8A) that are coupled to each other via commissures.

Bilateral Coordination of the Two CPGs on the Two Lateral Halves of the Brain Stem

Which projection neurons synchronize the fast and slow trill rhythms generated by the two CPGs in each half of the brain stem? We found that transection of the anterior commissure alone, the posterior commissure alone, and both commissures resulted in no delay (Fig. 4), some delay (Fig. 5), and no coordination (Fig. 3) between the left and right CAPs, respectively. In addition, the loss of the posterior commissure sometimes resulted in asynchronous fictive slow trills from the two sides of the brain stem, whereas fictive fast trills never became asynchronous (Fig. 5G). These results suggest that although the two commissures play a compensatory role in synchronizing the two CPGs on both sides of the brain stem, the posterior commissure likely plays a more dominant role than the anterior commissure in coupling the two CPGs.

A previous anatomical study identified four types of commissural interneurons contained in the anterior and posterior commissures of the brain stem of *X. laevis*. The anterior commissure includes axons of DTAM neurons that project to the contralateral DTAM (DTAM_{CDTAM}; Fig. 8B) and of neurons that decussate first to the contralateral DTAM and project to the contralateral n.IX-X (DTAM_{cn.IX-X}; Fig. 8B). The posterior commissure includes axons of n.IX-X neurons that project to the contralateral n.IX-X (n.IX-X_{cn.IX-X}; Fig. 8B) and the neurons that decussate to the contralateral n.IX-X and project to contralateral DTAM (n.IX-X_{CDTAM}; Fig. 8B) (Zornik and Kelley 2007). Because the slow trill CPGs are likely contained in n.IX-X (Fig. 8A), we propose that projection neurons that terminate in n.IX-X (n.IX-X_{cn.IX-X} and DTAM_{cn.IX-X}) couple the two slow trill CPGs (see Fig. 8A). Fast trill CPGs that span n.IX-X and DTAM, in contrast, are proposed to be coupled by a population of neurons that terminate in DTAM (n.IX-X_{CDTAM} and DTAM_{CDTAM}; Fig. 8A). Furthermore, we suggest that based on the degree of deterioration of bilateral synchrony observed upon transections, the coupling efficiency differs among these commissural interneurons. The n.IX-X_{cn.IX-X} and n.IX-X_{CDTAM} axons contained in the posterior commissure likely couple the rhythms generated by the fast and slow CPGs with maximum efficiency, because transection of these axons resulted in significant delay or desynchronization between the two halves of the fast and slow trill CPGs (Fig. 8A; coupling efficiency). DTAM_{DTAM} and DTAM_{cn.IX-X} axons contained in the anterior commissure couple the fictive fast trill and slow trill rhythms with minimum efficiency, because the loss of the anterior commissure has little impact on the synchronous activity of the two nerves during the fictive fast and slow trills (Fig. 8A). In this model, the commissural interneurons that couple the CPGs on the two sides synchronize the timing of the two oscillators by eliciting spikes from laryngeal motoneurons from the right and left brain stem near simultaneously. The loss of these commissural interneurons will result in either a delay between the rhythms generated by the two oscillators (Fig. 5, E and F) or autonomous operation of each oscillator (Fig. 5G).

Mechanisms for Fast and Slow Trill Initiation and Its Bilateral Synchronization

In the present study, transections of the projections between extended amygdala and DTAM, along with the anterior commissure, revealed mechanisms underlying fast and slow trill initiation that appear to be distinct.

Slow trill initiation. Previously, we have shown that bilateral transection between n.IX-X and DTAM eliminates fictive advertisement calls entirely. If the projections between n.IX-X and DTAM are only necessary for the fast trill generation, but not for slow trill CPGs, then why could we not elicit slow trills from any of the bilaterally transected brains? We suggest that there is a descending projection from DTAM to n.IX-X that initiates slow trill CPGs (see Fig. 8A); in the bilaterally transected brains, the signal to initiate the slow trill CPG is disrupted, even though the CPG itself is intact. Interestingly, a slow trill almost always follows a fast trill and is almost never produced in isolation both in vivo and in vitro. Thus it is possible that the completion of the fast trill may generate a signal that descends from DTAM to n.IX-X to initiate slow trills. Regardless, we suggest that unilateral input from DTAM to n.IX-X is sufficient to initiate slow trills, as we have observed in unilaterally transected brains (Fig. 2B), and the initiation of slow trills is bilaterally synchronized via anterior and posterior commissures (see Fig. 8A). Accordingly, any transection in this study that left one of the two commissures intact (unilateral DTAM to n.IX-X transverse transection, anterior commissure sagittal transection, posterior commissure sagittal transection, descending transverse input together with anterior commissure sagittal transection) resulted in synchronized initiation of fictive slow trills (Figs. 2B, 4B, 5B, and 6, B, F, and H), whereas the transection that eliminated both anterior and posterior commissure resulted in the autonomous initiation of fictive slow trills (Fig. 3, D and E).

Fast trill initiation. In brains in which both anterior and posterior commissures were transected, fictive fast trills from the two isolated sides of the brain stems were initiated, on average, within 100 ms of each other. The bath application technique used to apply 5-HT in the present study does not necessarily activate the two DTAM simultaneously, because the patterns of activation and desensitization of a population of receptors expressed by the two DTAMs are different, based on the geometric spread of the 5-HT solution through the recording chamber, or a population of neurons downstream of the 5-HT signaling has a different threshold for activation. Thus our results suggest the presence of a bilaterally synchronized descending signal from extended amygdala that initiates fictive fast trills from the two sides of the brain stem within a short time window (Fig. 3E).

It was puzzling, however, that our previous study showed that the elimination of the descending projections from extended amygdala to DTAM had no effect on the initiation of the fictive fast trills in response to 5-HT (see Fig. 7, D and E, for example), whereas in this study, we could decouple the initiation of fast trills from the two sides of the brain stem by transecting both the descending inputs to the brain stem and the anterior commissure. To explain these observations, we propose that exogenous 5-HT initiates fictive fast trills in two complementary ways. One way is to activate the extended amygdala, which sends bilateral-descending signals to left and

right DTAM simultaneously, resulting in near-synchronous activation of the fast trill CPG from the two sides (see Fig. 8C). The other way is to activate a population of neurons in DTAM unilaterally, which then projects to contralateral DTAM via the anterior commissures and results in simultaneous initiation of the fast trills from the two sides (see Fig. 8C). In the latter scenario, we speculate that each DTAM is activated by 5-HT independently. Under this scenario, unilateral activation of DTAM in brains without descending inputs (with intact anterior commissures) can still initiate fictive advertisement calling by both halves of the brain stem via the projection neurons connecting the two DTAMs through the anterior commissure (Fig. 8A). In brains with sagittal transection of anterior commissures (with intact descending inputs), activation of the extended amygdala by 5-HT generates bilaterally synchronized initiation signals that activate left and right DTAM to initiate advertisement calls from the two sides of the brain stem simultaneously. It is only when both of these projections are removed that fast trills are initiated by the left and right brain stem independently (Fig. 8A).

Of these two projection neuron populations, however, the anterior commissure projections appear to synchronize fictive fast trill onset more precisely than the bilateral projections from the extended amygdala, because the initiation of DTAM activity in the absence of anterior commissure (with or without posterior commissure) can result in a significant delay between the two sides (Figs. 3, D and E, and 7, J and L). Thus we propose that the extended amygdala signals that initiate fast trills from each side are permissive and allow fast trill initiations to take place but are not instructive in providing the timing information to initiate the fast trills.

Many episodic CPGs in vertebrates are considered to be initiated by the basal ganglia, with its major function being to “select” appropriate behavior at any given moment (Mink 1996; Nambu et al. 2002). Vocal CPGs of a variety of vertebrate species are also considered to be “selected” by the basal ganglia via periaqueductal gray (PAG) (Hikosaka 2007). The vocal initiation mechanisms of *X. laevis*, however, may be distinct from other CPGs. There has been no direct anatomical connections demonstrated between the PAG and the vocal nuclei nor has there been any demonstration of the involvement of basal ganglia for vocal initiation, to date, in *X. laevis*. Instead, DTAM (also known as parabrachial area) (Moreno and Gonzales 2005; Zornik and Kelley 2011) or pretrigeminal nucleus (Schmidt 1992) is reciprocally connected with the CeA, a nucleus included in extended amygdala, which is also reciprocally connected with PAG in *X. laevis* (Moreno and Gonzales 2005). The BNST, another nucleus included in the extended amygdala, directly projects to the dorsal raphe nucleus (Moreno et al. 2012), which sends serotonergic projections to n.IX-X and DTAM (Rhodes et al. 2007; Yu and Yamaguchi 2009, 2010). One study showed that the lesioning of CeA disrupts the production of vocal responses to females, whereas the lesioning of BNST decreases calling behavior in vivo in male *X. laevis* (Hall et al. 2013). This study suggests that CeA plays a role in eliciting vocalization in response to socially salient stimuli, whereas the BNST plays a role in initiating vocal activity in general. Previously, we have shown that the increase of the extracellular concentration of endogenous serotonin using a selective serotonin reuptake inhibitor elicits fictive advertisement calls by activating 5-HT_{2C} recep-

tors expressed in the raphe nucleus and n.IX-X (Yu and Yamaguchi 2010). Although transverse transection at the level of the rostral optic tectum did not allow us to identify which descending inputs play a role in initiating fast trills, we suggest that the BNST is a likely candidate nucleus that elicits fast trills from the brain stem.

ACKNOWLEDGMENTS

The authors thank Matt Wachowiak, Erik Zornik, Paulo Rodrigues, and two anonymous reviewers for helpful comments on this manuscript and Malorie Jahn, Brandon Fisher, Shannon Roghaar, and Faith Denzer for analyzing data.

GRANTS

Support for this work was provided by National Science Foundation 1146501 and start-up funds provided by the Department of Biology and USTAR at the University of Utah (to A. Yamaguchi).

DISCLOSURES

No conflicts of interest, financial or otherwise, are declared by the authors.

AUTHOR CONTRIBUTIONS

A.Y. conceived and designed research; J.C.B. and T.A. performed experiments; A.Y., J.C.B., and T.A. analyzed data; A.Y. interpreted results of experiments; A.Y. prepared figures; A.Y. drafted manuscript; A.Y. edited and revised manuscript; A.Y. approved final version of manuscript.

REFERENCES

- Albersheim-Carter J, Blubaum A, Ballagh IH, Missaghi K, Siuda ER, McMurray G, Bass AH, Dubuc R, Kelley DB, Schmidt MF, Wilson RJ, Gray PA. Testing the evolutionary conservation of vocal motoneurons in vertebrates. *Respir Physiol Neurobiol* 224: 2–10, 2016.
- Bass AH, Gilland EH, Baker R. Evolutionary origins for social vocalization in a vertebrate hindbrain-spinal compartment. *Science* 321: 417–421, 2008.
- Berkowitz A. Multifunctional and specialized spinal interneurons for turtle limb movements. *Ann N Y Acad Sci* 1198: 119–132, 2010.
- Briggman KL, Kristan WB Jr. Imaging dedicated and multifunctional neural circuits generating distinct behaviors. *J Neurosci* 26: 10925–10933, 2006.
- Brown TG. On the nature of the fundamental activity of the nervous centres; together with an analysis of the conditioning of rhythmic activity in progression, and a theory of the evolution of function in the nervous system. *J Physiol* 48: 18–46, 1914.
- Brown TG. The intrinsic factors in the act of progression in the mammal. *Proc R Soc Lond B* 84: 308–319, 1911.
- Buchanan JT. Flexibility in the patterning and control of axial locomotor networks in lamprey. *Integr Comp Biol* 51: 869–878, 2011.
- Cangiano L, Grillner S. Fast and slow locomotor burst generation in the hemispinal cord of the lamprey. *J Neurophysiol* 89: 2931–2942, 2003.
- Cangiano L, Hill RH, Grillner S. The hemisegmental locomotor network revisited. *Neuroscience* 210: 33–37, 2012.
- Chagnaud BP, Baker R, Bass AH. Vocalization frequency and duration are coded in separate hindbrain nuclei. *Nat Commun* 2: 346, 2011.
- Cohen AH, Harris-Warrick RM. Strychnine eliminates alternating motor output during fictive locomotion in the lamprey. *Brain Res* 293: 164–167, 1984.
- Cowley KC, Schmidt BJ. Effects of inhibitory amino acid antagonists on reciprocal inhibitory interactions during rhythmic motor activity in the in vitro neonatal rat spinal cord. *J Neurophysiol* 74: 1109–1117, 1995.
- Dickinson PS, Mecasas C, Marder E. Neuropeptide fusion of two motor-pattern generator circuits. *Nature* 344: 155–158, 1990.
- Evans BJ, Carter TF, Greenbaum E, Gvozdkik V, Kelley DB, McLaughlin PJ, Pauwels OS, Portik DM, Stanley EL, Tinsley RC, Tobias ML, Blackburn DC. Genetics, morphology, advertisement calls, and historical records distinguish six new polyploid species of African clawed frog (*Xenopus*, Pipidae) from West and Central Africa. *PLoS One* 10: e0142823, 2015.
- Fetcho JR, McLean DL. Some principles of organization of spinal neurons underlying locomotion in zebrafish and their implications. *Ann N Y Acad Sci* 1198: 94–104, 2010.
- Garcia AJ 3rd, Zanella S, Koch H, Doi A, Ramirez JM. Chapter 3—networks within networks: the neuronal control of breathing. *Prog Brain Res* 188: 31–50, 2011.
- Grillner S. Biological pattern generation: the cellular and computational logic of networks in motion. *Neuron* 52: 751–766, 2006.
- Hall IC, Ballagh IH, Kelley DB. The *Xenopus* amygdala mediates socially appropriate vocal communication signals. *J Neurosci* 33: 14534–14548, 2013.
- Hikosako O. GABAergic output of basal ganglia. In: *Progress in Brain Research*, edited by Teper JM, Abercrombie ED, and Bolam JP. Amsterdam, Netherlands: Elsevier, 2007, vol. 160, p. 209–226.
- Hinckley C, Seebach B, Ziskind-Conhaim L. Distinct roles of glycinergic and GABAergic inhibition in coordinating locomotor-like rhythms in the neonatal mouse spinal cord. *Neuroscience* 131: 745–758, 2005.
- Hooper SL, Moulins M. Cellular and synaptic mechanisms responsible for a long-lasting restructuring of the lobster pyloric network. *J Neurophysiol* 64: 1574–1589, 1990.
- Hooper SL, Moulins M. Switching of a neuron from one network to another by sensory-induced changes in membrane properties. *Science* 244: 1587–1589, 1989.
- Huang Z, Satterlie RA. Neuronal mechanisms underlying behavioral switching in a pteropod mollusc. *J Comp Physiol A* 166: 875–888, 1990.
- Jurgens U, Hage SR. On the role of the reticular formation in vocal pattern generation. *Behav Brain Res* 182: 308–314, 2007.
- Kiehn O, Dougherty KJ, Hagglund M, Borgius L, Talpalar A, Restrepo CE. Probing spinal circuits controlling walking in mammals. *Biochem Biophys Res Commun* 396: 11–18, 2010.
- Kwan AC, Dietz SB, Webb WW, Harris-Warrick RM. Activity of Hb9 interneurons during fictive locomotion in mouse spinal cord. *J Neurosci* 29: 11601–11613, 2009.
- Leininger EC, Kitayama K, Kelley DB. Species-specific loss of sexual dimorphism in vocal effectors accompanies vocal simplification in African clawed frogs (*Xenopus*). *J Exp Biol* 218: 849–857, 2015.
- Li WC. Selective gating of neuronal activity by intrinsic properties in distinct motor rhythms. *J Neurosci* 35: 9799–9810, 2015.
- Li WC, Roberts A, Soffe SR. Specific brainstem neurons switch each other into pacemaker mode to drive movement by activating NMDA receptors. *J Neurosci* 30: 16609–16620, 2010.
- Marder E, Bucher D. Central pattern generators and the control of rhythmic movements. *Curr Biol* 11: R986–R996, 2001.
- Marder E, Bucher D, Schulz DJ, Taylor AL. Invertebrate central pattern generation moves along. *Curr Biol* 15: R685–R699, 2005.
- Marder E, Calabrese RL. Principles of rhythmic motor pattern generation. *Physiol Rev* 76: 687–717, 1996.
- Meyrand P, Simmers J, Moulins M. Construction of a pattern-generating circuit with neurons of different networks. *Nature* 351: 60–63, 1991.
- Meyrand P, Simmers J, Moulins M. Dynamic construction of a neural network from multiple pattern generators in the lobster stomatogastric nervous system. *J Neurosci* 14: 630–644, 1994.
- Mink JW. The basal ganglia: focused selection and inhibition of competing motor programs. *Prog Neurobiol* 50: 381–425, 1996.
- Moreno N, Gonzalez A. Central amygdala in anuran amphibians: neurochemical organization and connectivity. *J Comp Neurol* 489: 69–91, 2005.
- Moreno N, Morona R, Lopez JM, Dominguez L, Joven A, Bandin S, Gonzalez A. Characterization of the bed nucleus of the stria terminalis in the forebrain of anuran amphibians. *J Comp Neurol* 520: 330–363, 2012.
- Moult PR, Cottrell GA, Li WC. Fast silencing reveals a lost role for reciprocal inhibition in locomotion. *Neuron* 77: 129–140, 2013.
- Nambu A, Tokuno H, Takada M. Functional significance of the cortico-subthalamo-pallidal ‘hyperdirect’ pathway. *Neurosci Res* 43: 111–117, 2002.
- Popescu IR, Frost WN. Highly dissimilar behaviors mediated by a multifunctional network in the marine mollusk *Tritonia diomedea*. *J Neurosci* 22: 1985–1993, 2002.
- Potter KA, Bose T, Yamaguchi A. Androgen-induced vocal transformation in adult female African clawed frogs. *J Neurophysiol* 94: 415–428, 2005.
- Rhodes HJ, Yu HJ, Yamaguchi A. *Xenopus* vocalizations are controlled by a sexually differentiated hindbrain central pattern generator. *J Neurosci* 27: 1485–1497, 2007.
- Roberts A, Li WC, Soffe SR. A functional scaffold of CNS neurons for the vertebrates: the developing *Xenopus laevis* spinal cord. *Dev Neurobiol* 72: 575–584, 2012.
- Sakurai A, Gunaratne CA, Katz PS. Two interconnected kernels of reciprocally inhibitory interneurons underlie alternating left-right swim motor

- pattern generation in the mollusk *Melibe leonina*. *J Neurophysiol* 112: 1317–1328, 2014.
- Satterlie RA.** Reciprocal inhibition and postinhibitory rebound produce reverberation in a locomotor pattern generator. *Science* 229: 402–404, 1985.
- Satterlie RA.** Toward an organismal neurobiology: integrative neuroethology. *Integr Comp Biol* 53: 183–191, 2013.
- Schmidt RS.** Neural correlates of frog calling: production by two semi-independent generators. *Behav Brain Res* 50: 17–30, 1992.
- Sweeney LB, Kelley DB.** Harnessing vocal patterns for social communication. *Curr Opin Neurobiol* 28: 34–41, 2014.
- Tobias ML, Evans BJ, Kelley DB.** Evolution of advertisement calls in African clawed frogs. *Behaviour* 148: 519–549, 2011.
- Van Vreeswijk C, Abbott LF, Ermentrout GB.** When inhibition not excitation synchronizes neural firing. *J Comput Neurosci* 1: 313–321, 1994.
- Wang XJ, Rinzal J.** Alternating and synchronous rhythms in reciprocally inhibitory model neurons. *Neural Comput* 4: 84–97, 1992.
- Wang XJ, Rinzal J.** Spindle rhythmicity in the reticularis thalami nucleus: synchronization among mutually inhibitory neurons. *Neuroscience* 53: 899–904, 1993.
- Weimann JM, Marder E.** Switching neurons are integral members of multiple oscillatory networks. *Curr Biol* 4: 896–902, 1994.
- Yager DD.** A unique sound production mechanism in the pipid anuran *Xenopus borealis*. *Zool J Linn Soc* 104: 351–375, 1992.
- Yamaguchi A, Kelley DB.** Generating sexually differentiated vocal patterns: laryngeal nerve and EMG recordings from vocalizing male and female African clawed frogs (*Xenopus laevis*). *J Neurosci* 20: 1559–1567, 2000.
- Yu HJ, Yamaguchi A.** 5-HT_{2C}-like receptors in the brain of *Xenopus laevis* initiate sex-typical fictive vocalizations. *J Neurophysiol* 102: 752–765, 2009.
- Yu HJ, Yamaguchi A.** Endogenous serotonin acts on 5-HT_{2C}-like receptors in key vocal areas of the brain stem to initiate vocalizations in *Xenopus laevis*. *J Neurophysiol* 103: 648–658, 2010.
- Zornik E, Katzen AW, Rhodes HJ, Yamaguchi A.** NMDAR-dependent control of call duration in *Xenopus laevis*. *J Neurophysiol* 103: 3501–3515, 2010.
- Zornik E, Kelley DB.** A neuroendocrine basis for the hierarchical control of frog courtship vocalizations. *Front Neuroendocrinol* 32: 353–366, 2011.
- Zornik E, Kelley DB.** Regulating breathing and calling in an aquatic frog: neuronal networks in the *Xenopus laevis* hindbrain. *J Comp Neurol* 501: 303–315, 2007.

